

Bayesian Optimization with Directionally Constrained Search

Yang Li, Yaqiang Yao,

Abstract— Bayesian optimization offers a flexible framework to optimize an objective function that is expensive to be evaluated. A Bayesian optimizer iteratively queries the function values on its carefully selected points. Subsequently, it makes a sensible recommendation about where the optimum locates based on its accumulated knowledge. This procedure usually demands a long execution time. In practice, however, there often exists a computational budget or an evaluation limitation allocated to an optimizer, due to the resource scarcity. This constraint demands an optimizer to be aware of its remaining budget and able to spend it wisely, in order to return as better a point as possible. In this paper, we propose a Bayesian optimization approach in this evaluation-limited scenario. Our approach is based on constraining searching directions so as to dedicate the model capability to the most promising area. It could be viewed as a combination of local and global searching policies, which aims at reducing inefficient exploration in the local searching areas, thus making a searching policy more efficient. Experimental studies are conducted on both synthetic and real-world applications. The results demonstrate the superior performance of our newly proposed approach in searching for the optimum within a prescribed evaluation budget.

Index Terms—Bayesian Optimization, Gaussian Process, Expected Improvement, Directional Constraint.

1 INTRODUCTION

MACHINE learning is rarely optimization-free. Traditional numerical optimizers make use of the structural properties of the problems like convexity, submodularity etc. to accelerate their convergence rates. However, there are also a number of problems that traditional optimizers are insufficient. A typical example is tuning the hyper-parameters for some machine learning algorithms such that the validation error is minimized. In such a problem, there is no closed-form for the objective function, not to mention its structural properties. The hyper-parameters, which are considered as nuisances, need to be repeatedly changed and compared. When the objective function is computationally prohibitive to be executed repeatedly, traditional numerical optimizers become insufficient. Bayesian Optimization (BO) [1] offers a choice for such *black-box* problems, and has achieved a decent performance on a number of challenging benchmark functions [2].

For continuous objective functions, Bayesian optimization typically works by presuming the uncertainty of not-yet observed function values follows a multivariate Gaussian distribution. As new observations are made, it updates the belief about global minimizer and infers the next point that should be queried. For instance, in the problem of tuning the hyper-parameters of a machine learning algorithm, BO treats it as a global searching on an expensive, black-box function plane, whose derivatives are inaccessible. The algorithm of interest is invoked under different hyper-parameter settings. As more experimental results are observed, BO recommends a setting with high probability that will achieve a high performance based on its previous trails and accumulated knowledge.

BO is an iterative procedure that successively queries function values and updates a posterior distribution for not-yet evaluated points. Its performance depends critically on the strategy of selecting the next query point since this step enables it to actively learn the structure of the black-box function. This strategy is explicitly expressed via an *acquisition function*, which measures how much improvement or utility a not-yet-evaluated point would bring if it were selected.

Acquisition function distinguishes different Bayesian optimization techniques. A list of most popular ones include: Expected Improvement (EI) [1] over the present best result; Upper Confidence Bound (UCB) [3]; Probability of Improvement (PoI) [4], which introduces a parameter κ to trade-off exploring against exploiting. By exploitation, we mean that an algorithm always query a point that is most likely to be the optimum from its knowledge, without considering the ones that are associated with great uncertainties. Exploration, on the other hand, aims at reducing uncertainties on not-evaluated points. EI and UCB have demonstrated their efficiencies on finding the global optimum of multi-modal black-box functions [5], [6]. Other particularly successful designs are Entropy Search (ES) [7] and Predictive Entropy Search (PES) [8], [9], both of which involve maximizing the mutual information between a query point and a guess on the global minimizer.

All the above approaches are effective in the sense they will ultimately locate the global optimum, provided unlimited evaluation time. However, due to resource scarcity such as high-performance computers, evaluation time and even patience of practitioners, most BOs are executed within a given permissible number of iterations or *evaluation budget*. As a result, those approaches still keep a high level of exploring even when they are near the maximum iteration limit. This leads to a resource waste and excessively oscillat-

• The authors are with School of Computer Science and Technology, University of Science and Technology of China (USTC), Hefei, Anhui 230027, China. E-mail: {csly, yaoyaq}@mail.ustc.edu.cn

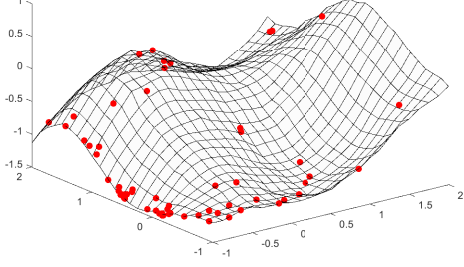


Fig. 1. The query points selected by Expected Improvement (EI) on a non-convex surface. Although some queries are actually near the global minimizer, there is still a large amount of trails jiggling around, bring no benefits but leading to a waste of evaluation budget. This oscillating behavior near the minimizer is what we want to avoid.

ing behavior on both the global and local scales. An example in Fig. 1 elucidates how this affects the behavior of a BO algorithm.

To reduce the oscillating behavior often needs assistance from the structural properties of the objective function, in particular the gradients. However, as we are dealing with a black-box problem, we cannot assume that its gradient information is accessible even locally. An immediate intuition is that, along with the execution of an optimizer, a global profile or a surrogate model about the objective function is made more and more accurate. We notice that, while it is not possible to utilize the gradients, we may extract some directional information from this constructed surrogate model, and encode our preference on the searching directions into the acquisition function of a BO algorithm.

In this work, we focus on the scenario where evaluation budget exists, and propose an approach that imposes a directional constraint with increasing effects on the searching policy. The whole procedure has several appealing properties: (1) At the early steps of an optimization, an optimizer is allowed to select the next query point freely by maximizing its acquisition function. (2) However, since there is a strict limit on the number of iterations or executions, it selects the next point to be evaluated from a direction that is more likely to yield decrease. Besides that, we include another requirement for this searching direction: it should span an acute angle with the last one on an optimization path. This requirement is imposed for the prevention of jiggles. (3) At the later stage especially near the end of iterations, this optimizer gradually dedicate most of its probability into a local searching in the most promising region as it becomes more rewarding. (4) This directional constraint takes effects in the form of probability gradually over the execution of an algorithm. Thus, our approach could be viewed as a novel combination of both global and local searching policies.

We will focus our discussion on a typical acquisition function: Expectation Improvement (EI), as it has been shown to be well-behaved and widely used [10]. Different from the method UCB, it does not own any tuning parameters. In addition, its simplicity on formulation is an appealing characteristic on perception. But we will show that our newly proposed constraint could easily be included

into most common probabilistic acquisition functions like EI, PoI, and UCB.

This paper is organized as follows. In Section 2, we list Gaussian process, Bayesian optimization, and expected improvement as a particular example of acquisition functions. Section 3 introduces the directional constraint and outlines the optimization procedure under the effects from this newly proposed constraint. The experimental results and discussions are then presented in Section 4, showing our approach is more efficient than existing methods. Finally, section 5 concludes the paper and present future work, while Appendix lists the technical details that are omitted in the text.

2 BACKGROUND

2.1 Gaussian Process

A Gaussian Process (GP) is defined on a uncountable set of random variables. Any selected variables from this set are subject to a joint Gaussian distribution. Formally, data set \mathcal{D} is a collection of n points of dimension d , $X = \{x_1, x_2, \dots, x_n\}$. The corresponding real-valued function values are denoted by $f(X) = \{f(x_1), f(x_2), \dots, f(x_n)\}$. A functional viewpoint treats GP as a distribution defined over functions [11], which compactly describes the uncertainty on $f(\cdot)$ via a mean function $\mu(\cdot)$ and a covariance kernel $k(\cdot, \cdot)$. Some key properties such as stationarity, smoothness etc. are specified through the covariance function. For instance, a hyper-parameter θ is routinely included in the covariance function for the sake of versatility, which controls its kernel width:

$$k(x_i, x_j) = \exp\left(-\frac{1}{2\theta}\|x_i - x_j\|\right) \quad (1)$$

Let x' denotes an arbitrary query point. The GP tells us that the joint distribution of function values on the query point and the collection of samples should satisfy:

$$\begin{bmatrix} f(X) \\ f(x') \end{bmatrix} \sim \mathcal{N}\left(\begin{bmatrix} \mu(X) \\ \mu(x') \end{bmatrix}, \begin{bmatrix} k(X, X) & k(X, x') \\ k(x', X) & k(x', x') \end{bmatrix}\right)$$

where the operations should be understood as elementwisely on their matrix inputs. $\mathcal{N}(\cdot)$ is a multi-variate Gaussian distribution.

The posterior distribution on the query point x' is calculated by standard Bayesian rules. The distribution for the function value on x' , which is represented as $f(x') \sim p(f(x')|x', X, f(X))$, can be calculated as:

$$\begin{aligned} f(x') &\sim p(f(x')|X, f(X), x') \\ &= \mathbb{E}_{p(f(X)|X)} p(f(x')|X, f(X), x') \\ &= \mathcal{N}(\mu(x'), \Sigma(x')) \end{aligned}$$

where

$$\begin{aligned} \mu(x') &= \mu(x') + k(x', X)k(X, X)^{-1}(f(X) - \mu(X)) \\ \Sigma(x') &= k(x', x') - k(x', X)k(X, X)^{-1}k(X, x') \end{aligned} \quad (2)$$

Being viewed as a machine learning algorithm, GP uses a measure of similarity to make prediction on an unseen point. As opposed to a traditional point estimation, this prediction comes along with uncertainty or a marginal distribution.

2.2 Bayesian Optimization

Bayesian Optimization (BO) offers a framework for finding the extrema of an objective function:

$$\min_x f(x) \quad (3)$$

where $f(x)$ is reckoned prohibitively expensive to be executed for many times. Moreover, in the case of black-box problems, one does not have a closed form but may only query its values at sampled points. As those evaluations are costly, $f(\cdot)$ should be invoked as few as possible.

Any Bayesian method depends on a prior distribution. By thinking of GP as the prior probability on functions, as analogous to random variables, this prior represents our beliefs over the space of all feasible objective functions [12]. By doing this, the undetermined function values on non-yet evaluated points are expressed through a probabilistic distribution. The benefits of this Bayesian reformulation are obvious. The GP can iteratively incorporate new information and updates its beliefs on the unevaluated points. These steps are comparatively cheap. Hence, at each iteration, there is no need to execute the objective function on all candidate points. We only pick out the most promising one for the next evaluation according to some criterion. In this way, we restrict the computations of costly objective function to only on the selected points. Next, GP updates the posterior beliefs on all the points that are waiting for evaluations.

A BO algorithm starts with two randomly chosen points. At each step, an *acquisition function* is maximized to determine the next point to evaluate, which models the utilities and rewarding of not-yet evaluated points based on the history information. The next point is then chosen on the *argmax* of this function. The new pair, denoted by $(x^+, f(x^+))$, are brought into a library of evaluated set and reduces the uncertainty around x^+ . The posterior distribution over the function space is updated and the whole process is repeated. A nice property is that a BO algorithm can always return a recommended point if it were to stop without notice.

2.3 Expected Improvement

The above procedure of BO holds with a key step, i.e. the selection of a most promising point. The policy of actively selecting next point highly affects the performance of an optimizer. A natural and popular one is the *Expected Improvement* (EI) [1] which estimates the gains of query points and always selects the one that yields most decrease. In other words, the selected point is thought to gain the most advance towards the optimum.

To begin with, we first define some notations that would be useful throughout our paper. Let \tilde{x} be the best point achieved so far.

$$\tilde{x} = \operatorname{argmin}_{\mathcal{T}} f(x) \quad (4)$$

where \mathcal{T} denotes the evaluated point set. We represent all points by Ω . In principle, the new point to be evaluated, denoted by x^+ , is expected to lie around $\operatorname{argmin}_{x \in \Omega/\mathcal{T}} f(x)$, with Ω/\mathcal{T} represents the not-yet evaluated candidate set.

The EI is defined through a relative decrease of $f(x)$ on a point x against the minimal point \tilde{x} tested till far. Due to

the GP hypothesis on the unexplored points, this quantity is itself a random variable and is defined as:

$$I(x) = \max\{0, f(\tilde{x}) - f(x)\} \quad (5)$$

and EI quantity is obtained by taking expectation on both sides.

$$\mathbb{E}[I(x)] = \mathbb{E}[I(x)|\mathcal{T}, x] \quad (6)$$

An easy way to compute the above EI acquisition function was derived in [13]:

$$EI(x) = \Sigma f(x)(Z\Phi(Z) + \phi(Z)) \quad (7)$$

in which an intermediate variable Z is given as $Z = \frac{\mu(x) - f(\tilde{x})}{\Sigma(x)}$. Φ and ϕ are the standard normal cumulative distribution function (CDF) and probability density function (PDF), respectively.

Under only a weak regularity condition, BO based on EI could converge to the global optimum. Its drawback on the behavioral aspect is that it concentrates more on exploitation. Points that have high probabilities of being greater than $f(\tilde{x})$ are more preferable than points that with great uncertainty, even though the latter may have a chance to get larger gains. In other words, EI is a greedy sampler in a long run. Likewise, Probability of Improvement (PoI), and Upper Confidence Bound (UCB) are also focusing on maximizing the probability of rewarding in picking the next point but UCB leaves the trade-off between exploration and exploitation to the user. The entropy-based policies e.g. Entropy Search (ES) and Predictive Entropy Search (PES) mainly explore the unknown areas in order to reduce the uncertainty about the location of the optimum. In this study, we adopt EI as basic acquisition function. In our scenario where number of execution iterations is fixed in advance yet usually insufficient for most BO, the greedy behavior of EI is of least concern to us.

Beside EI, many other acquisition functions have been proposed for various scenarios. To decide the next point under inequality constraints, Gardner et al. [14] proposed an acquisition function as the product of EI and the probability of meeting feasibilities of all the constrains. This latter was realized by assuming the independences among constraints. Other attempts include modifying the objective function in order to add a penalty on constraint violations, punishing the unfeasible recommendations made by the acquisition function. By doing so, these works managed to remove the constraints from the original problems. For instance, Lee et al. [15] constructed an auxiliary function by making use of augmented Lagrangian formulation. This technique was extended on handling both the inequality and equality constraints [15]. Bernardo et al. [16] studied the scenario where the constraint functions are not easily formulated. They worked around this problem by approximating the unknown function so as to estimate the probabilities of meeting the constraints. A key update is the proposal of a new integrated improvement-based criterion conditional on all responses from the input. This quantity is computed over the entire point space. Likewise, the acquisition function in [17] quantifies the expected reduction of the uncertainty below the best one found so far. Both quantities need integrating throughout the feasible points. Lam et al. [18],

[19] model the future utilities by looking ahead. The long-term rewards in the finite-budget scenario are built through dynamical programming over future steps. However, the lookahead strategy needs more invocations of objective function otherwise the rewards would come with great uncertainties.

In summary, all the methods are mainly focusing on carefully processing the objective function and constraints such that they can be both handled in a same scheme. Few considers the scenario with a finite budget on the number of invocations of the objective function. In this case, an optimizer needs to be aware of the remaining budget so as to balance the trade-off between exploration and exploitation in a principled way.

3 DIRECTIONAL CONSTRAINT

We are seeking for a BO method, being executed in cases with a limited evaluation budget, to return as minimal a value as possible. An algorithm is required to choose samples wisely by assessing the remaining budget. A general idea is that an algorithm should be more aggressive on exploitation when it is approaching the evaluation limit. Most probability should be assigned to local exploitation in the most promising area. This is reasonable as it has undergone a wide exploration and has a good chance to locate a promising region where an optimum is likely to be found. However, this intuition cannot be captured by the simple EI since it will not take the evaluation budget into account.

Motivated by the above analysis, we reformulate the acquisition function with a finite evaluation budget as a product of EI and a local searching policy (obtained through considering the neighboring evaluated points). These two terms are balanced conditional on the remaining evaluation budget. The final acquisition function is formulated as:

$$H(x)^{\rho(t)} [\max\{0, f(x^+) - f(\tilde{x})\}]^{1-\rho(t)} \equiv H(x)^{\rho} EI(x)^{1-\rho(t)} \quad (8)$$

$H(x)$ models the utilities of all possible searching directions pointing from present x_t , which is denoted as $g = \frac{x - x_t}{\|x - x_t\|}$. This quantity to the power of ρ is multiplicatively combined with EI. The power ρ increasingly changes in the range of $[0, 1]$. An implicit premise associated with the above formulation is the separability between the objective function and the directional constraint, which is reasonable since directions have an analogous role to the gradient. This statistical quantity $H(x)$ serves a similar role in constraining searching directions in order to refine the exploring behavior. We refer to this newly proposed directional statistics as *directional constraint* in order to distinguish it from the normal ones. Before introducing the design of $H(x)$, we first look at an extension and properties of the step function $\rho(t)$.

As we can observe, EI is a probability quantity measuring the utility of a sample from the not-yet evaluated point set. Any other probabilistic models are equally feasible. This makes the constraint widely applicable for a range of utility models. For instance, in the constrained BO, the utility model could employ an augmented EI quantity:

$$EI(x) \equiv C(x) \max\{0, f(x^+) - f(\tilde{x})\} \quad (9)$$

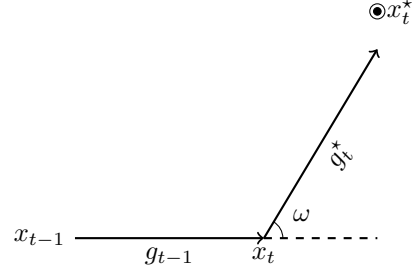


Fig. 2. This figure illustrates the directional adherence between two successful steps in the BO. Provided x^* is the ideal point that EI suggests and that g_{t-1} is the last searching direction, a conventional searching policy of BO would pick x^* since it has the highest probability to decrease. However, the uncertainty of GP provides the source for jiggles on a local scale. Therefore, in our approach, we complement the conventional searching policy by proposing a constraint on the direction of actual move. This statistical quantity g_t is demanded to be positively correlated with the past origination g_{t-1} . Intuitively, it requires that an angle ω between g_t and g_{t-1} is strictly less than 90 degrees.

where, the term $C(x)$ is the product of probabilities of meeting the feasibilities of equality or inequality constraints.

The trade-off between EI and directional constraint is controlled by the step function $\rho(t)$, whose changing pattern affects the behavioral aspects of an optimizer. As we can expect, the setting of $\rho(t)$ is problem-dependent and, to some extent, related to the evaluation budget. In our study, for simplicity, we restrict our discussion to the simplest design, i.e. ρ changes linearly with iterations: in t -th iteration

$$\rho(t) = \frac{t}{T}, \quad t = \{0, \dots, T\} \quad (10)$$

in which T denotes the number of evaluations.

3.1 Modeling Searching Directions

We have rectified the EI by augmenting a directional constraint with $\rho(t)$ as its exponent. Our remaining issue is to model the utilities of all searching directions. We again turn to approximation and Bayesian formalism for a feasible and easy way. However, searching directions are a new type of input for the BO. Modeling the directional probability as Gaussian distribution becomes problematic.

Specifically, we are concerned with modeling the adherence to a past direction or originations in the BO, hoping to achieve a consistent decrease on a local scale. To do so, we need to solve two issues: (1) The way to specify an adherence or consistence to the past direction. (2) A full Bayesian treatment of directions which relies on devising an iterative update Bayesian rules for directional statistics.

Without loss of generality, we assume that two neighboring samples are x_t and x_{t-1} . The “optimal” point recommended by the GP is denoted as x_t^* . All points come from a real-valued vector space \mathbb{R}^d . The direction pointing from x_{t-1} to x_t is denoted as g_{t-1} . The direction from x_t to x_t^* is referred to as g_t . The positional relations between points are illustrated in Fig. 2.

To begin with, let us revisit a limitation possessed by a conventional searching policy of BO. When it suggests a point x^* based on the estimated probability from GP and/or the benefit in a long run, due to the smoothness of GP, we actually get a distribution of “best” points. However,

the points in the vicinity of x^* are totally neglected by the conventional optimizers, which have also a great chance get a high reward. This discovery permits us to design a more effective searching policy by considering the distribution rather than the point itself.

Due to the uncertainties on the responses, the probability estimated from GP is severely discounted. This gives the source to the jiggles and inefficient probing on a local scale. To alleviate this problem, we introduce an additional constraint for g_t , i.e. the angle between g_t and g_{t-1} is enforced to be acute. This condition enforces the searching direction g_t to be adherent to the last one and not reversed, with the hope for an adherent optimization path and a resultant consistent decrease. This requirement is illustrated in Fig. 2.

To devise an iterative update Bayesian rules, however, is not an easy task as we are modeling points with GP in an Euclidean space. It is challenging to build a model on the directions directly. The directional data have a unit norm and are assumed to live in the surface of a hypersphere. To model this new type of data, in this study, we make use of Von Mises-Fisher distribution (Vmf) from directional statistics [20], which is defined on $(d - 1)$ -dimensional hypersphere in \mathbb{R}^d .

$$Vmf(g|\theta, \kappa) = C_d(\kappa) \exp(\kappa \theta^T g) \quad (11)$$

where $\|g\| = 1, g \in \mathbb{R}^d, \kappa > 0, \kappa \in \mathbb{R}$ and $\|\theta\| = 1, \theta \in \mathbb{R}^d$. The parameters θ and κ represent the averaged direction and concentration parameter, respectively. In particular, the greater the value of κ , the higher concentration the probability mass is around the mean direction. The distribution is uniform on the sphere when $\kappa = 0$. The normalization constant $C_d(\kappa)$ satisfies

$$\int_{\|x\|=1} \exp(\kappa \theta^T x) dx = \frac{(2\pi)^{d/2-1} B_{d/2-1}(\kappa)}{\kappa^{d/2-1}} \equiv C_d(\kappa)$$

where B_p is a modified Bessel function of order p . If $d = 2$ the distribution reduces to the von Mises distribution (aka. circular normal distribution) on a circle.

We take termination from Bayesian formalism. The first step is to cast the points in the Euclidean space to the elements on the sphere. This is easy as we are dealing with points along an optimization trace. The directional statistics is built through the directions along the optimization trace as shown in Fig. 2. The prior probability on g_t is assumed to be centered around θ_t with concentration parameter κ_t :

$$H_t(x) \triangleq Vmf(g_t|\theta_t, \kappa_t) \quad (12)$$

where $g_t = \frac{x - x_{t-1}}{\|x - x_{t-1}\|}$. Note that the time stamp is added as subscript to $H(x)$ for clarity.

We approximate the posterior distribution $p(g_{t+1}|x_{t+1})$ via a function of same form $Vmf(g_{t+1}|\theta_{t+1}, \kappa_{t+1})$, where θ_{t+1} and κ_{t+1} are unknown parameters waiting to be inferred.

Moving from x_t to x_{t+1} , GP updates our belief about the response surface in the region surrounding x_{t+1} and delivers an updated x_{t+1}^* . We should modify the searching direction g_{t+1} accordingly. Hence, at time $t + 1$, we have the past orientation g_t and updated g_{t+1}^* which starts from x_{t+1} and ends at x_{t+1}^* . We turn to Bayesian rules with the hope

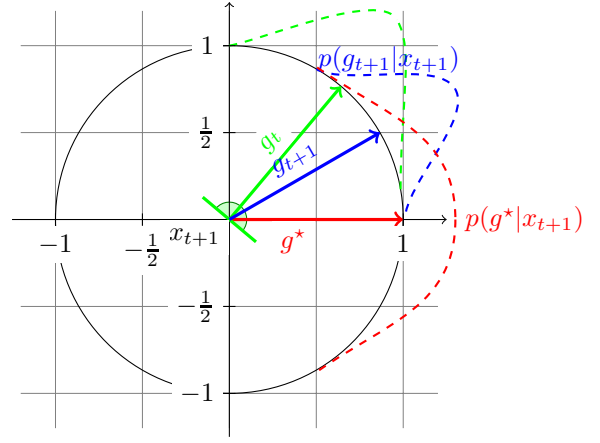


Fig. 3. A schematic diagram to infer the posterior distribution of searching directions at step $t + 1$. In this diagram, the past direction g_t in green and the direction suggested by GP in red are synthesized to compute the posterior distribution for g_{t+1} . In order to maintain the adherence and consistency to an optimization path, the inconsistent part in the distribution of g^* is pruned, with the hope to avoid the jiggles in the local search.

to synthesize two knowledges. The posterior distribution is computed as follows:

$$\begin{aligned} H_{t+1}(x) &= p(g_{t+1}) \\ &= \int dg_t^* dg_t \mathbb{I}(\langle g_{t+1}, g_t \rangle \geq 0) p(g_t) p(g_{t+1}|g_t^*) p(g_t^*) \end{aligned} \quad (13)$$

where $g_{t+1} = \frac{x - x_t}{\|x - x_t\|}$.

In the above Eq. (18), we enforce the adherence to hold by adding condition $\mathbb{I}(\langle g_t, g_{t+1} \rangle \geq 0)$, where $\mathbb{I}(\cdot) = 1$ when $\langle g_t, g_{t+1} \rangle \geq 0$ holds, otherwise $\mathbb{I}(\cdot) = 0$. We illustrate this idea in Fig. 2. The point x^* is the point GP suggests on step $t + 1$. These two points x_t and x_{t+1} , together with x_{t+1}^* consist an optimization path. The jiggle happens when the new searching direction g_{t+1} deviates much from the past orientation or even reverses to g_t . This condition exists to alleviate the jiggles in the update rules for g_{t+1} by only considering g_{t+1} that spans an acute angle with g_t . Overall, $H(x)$ guarantees that these two steps passing through are adhering to an optimization path and thus may lead to a consistent decrease. This general idea is graphically illustrated in Fig. 3.

The parameter κ_{t+1} of VMF represents how the directions disperse on the sphere. As we have already noticed, there is no closed-form for the posterior estimation of κ . We again refer to approximation for an easy way to compute this random quantity. To facilitate presentation, we move the technically cumbersome proof to Appendix. An easy way in the 2D case is presented below.

When $d = 2$, corresponding to the case we are optimizing in a flat plain. The parameters θ_{t+1} and κ_{t+1} are updated as:

$$\begin{aligned} \kappa_{t+1} &= \frac{1}{4} \sqrt{\hat{\kappa}^* \kappa_t (\hat{\kappa}^{*2} + \kappa_t^2 - 8 + 16\kappa_t^2)} \\ \theta_{t+1} &= \frac{k}{\sqrt{1 + k^2}} g_{t+1}^* + \frac{1}{\sqrt{1 + k^2}} g_t \end{aligned} \quad (14)$$

where $k = \frac{1}{4\kappa_t} \sqrt{\hat{\kappa}^* \kappa_t (\hat{\kappa}^{*2} + \kappa_t^2 - 8)}$ balances between g_{t+1}^* and past direction g_t . More details including the descrip-

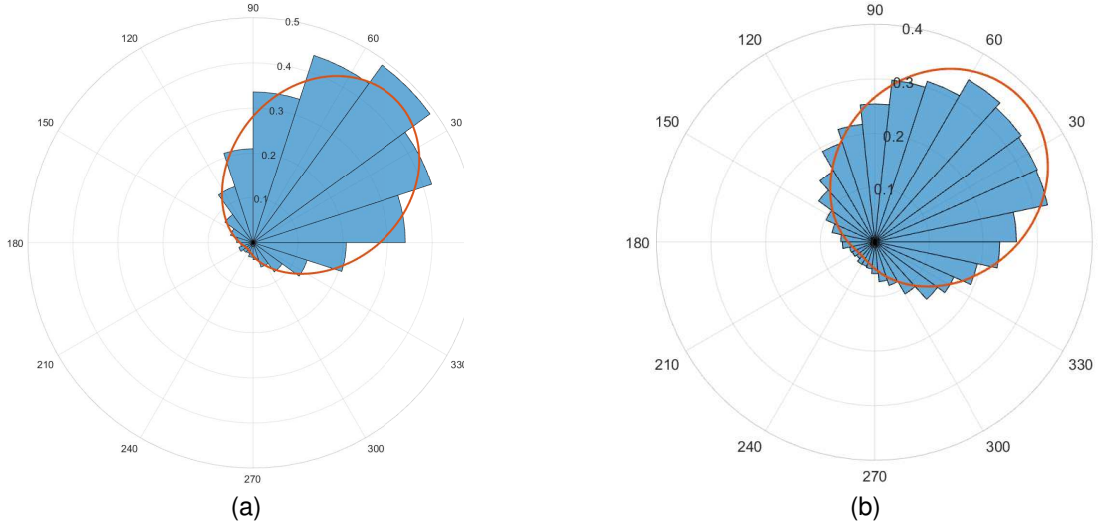


Fig. 4. The circular histogram for both prior and posterior distribution. The left panel (a) displays the statistics along with the true circular distribution enveloping the bars. The right panel (b) displays the approximated posterior distribution in the form of Vmf . From the figure, it can be concluded that, in our current experimental setting, Vmf is an appropriate PDF choice. Moreover, the approximated probabilities through Bayesian rules matches the true posterior distribution.

tions of variables are given in Appendix. In principle, these update rules make κ self-adaptive, which could be quite helpful when the algorithm is exploring a rugged target surface.

4 EXPERIMENT

We evaluate our method on several problems: three synthetic tasks and two real-world datasets. We implemented our method on the basis of GP. All GP hyper-parameters were selected under the criterion of maximizing the marginal likelihood.

4.1 Evaluation Criterion

To compare the performances of different Bayesian optimizers, we use utility gap metric [8]. At iteration n , this metric measures the gap between the optimal function value $\min(f)$ and the value of objective function at a recommended point \tilde{x}_n of step n . Recall that $\tilde{x}_n = \operatorname{argmin}_{\mathcal{T}} f(x)$, where \mathcal{T} is evaluated point set till iteration n .

$$e_n = \begin{cases} |f(\tilde{x}_n) - \min(f)| & \text{if } \tilde{x}_n \text{ is feasible.} \\ |\Psi - \min(f)| & \text{otherwise.} \end{cases} \quad (15)$$

where Ψ a penalty function when the optimizer recommends an infeasible point or makes no recommendation. Ψ could be any large real-valued constant greater than $\max f(x)$. The recommended point \tilde{x}_n is different from the one selected for testing at step n . The recommended point is the best point seen so far by the optimizer. In other words, if the optimizer were stopped at step n , this point would be the most promising one. If the function optimum $\min(f)$ is inaccessible, we use the magnitude of function at \tilde{x}_n instead as we are doing minimization.

4.2 Synthetic Problems

Simulation 1

We begin with one synthetic data generated according to VMF distribution. We verify the agreement between the Bayesian update rules (detailed in Appendix) and the results estimated from samples. This numerical experiment is to verify the precision as we make approximations during the calculation of posterior probability. In this simulation, the prior knowledge of g_t took the form of Vmf , whose $\kappa = 1$ and mean direction as $\theta = 1$. The g^* was sampled from an isotropic Gaussian distribution with $[1, 1]^T$ as its mean vector and $[1.5, 1.5]^T$ as the covariance diagonals. We took 10000 samples from this distribution to estimate the intermediate variable \hat{R} . The posterior distribution was assumed to take the form of $Vmf(\cdot)$. g_{t+1} is generated under the constraint that $\langle g_{t+1}, g_t \rangle > 0$, such that we do not need to consider the trivial case in Eq. (18). The circular histogram depicts the distribution of samples in a polar coordinate system. The enveloping curve around the circular histogram indicates the continuous probability density function (PDF) computed through Bayesian approximation. We scaled the PDF for the convenience of comparison.

By looking at the Fig. 4b, one can observe two phenomena: (1) Loosely speaking, the observed orientations generated under the constraint of acute angle normally coincide with the Vmf . Hence, it is reasonable for the assumption for the PDF of post-data probability being taken as Vmf , at least in this simplified simulation setting. (2) The PDF calculated by our method, as compared with sample histogram, confirms the general agreement between the estimated distribution and a *posteriori* circular histogram for observations, although not ideally. If considering the computational efficiency, the estimated PDF used in this scenario exhibits a great advantage. We will return to investigate the effects of approximations on the overall performance in later simulations.

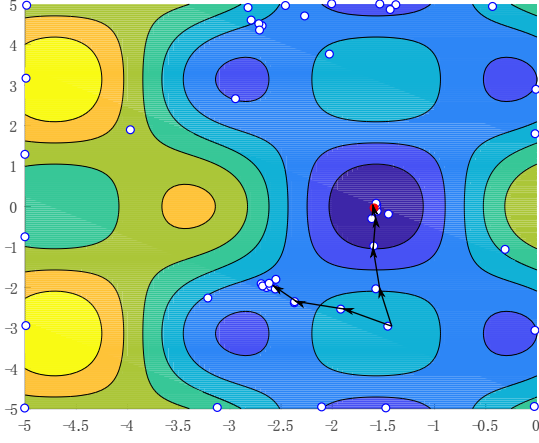


Fig. 5. The DCBO trace under no constraint. Fifty evaluations are permitted. We connect two successive optimization paths by arrows. We can see that, near the end of iterations, the searching does not disperse over the whole space but reduce to a local behavior.

Simulation 2

In this simulation, we adopt one synthetic problem, which is a two-dimensional continuous and multi-modal function. It has been commonly used as a benchmark problem for global optimization methods [14]. In this experiment, an optimizer is searching over the response surface for the global minimum. Its effectiveness is evaluated not merely through whether this optimizer manages to locate the optimum within a limited execution budget, but also depends on how it balances the exploitation and exploration within the execution process to speed-up the searching. The latter obviously determines its overall performance.

In this simulation, the execution budget was setup to be fifty iterations, or at most fifty invocations of target functions. The searching is restricted within a rectangular area, $[-5, 0] \times [-5, 5]$. The response surface is a 2D plate, and the objective function is described by the following formula:

$$\mathcal{O}(x, y) = \cos(2x) \cos(y) + \sin(x) \quad (16)$$

Besides, this problem could be more challenging by adding a constraint that splits the rectangular area into multiple feasible bands. The constraint is formulated as in Eq. (17).

$$c(x, y) = \cos(x) \cos(y) - \sin(x) \sin(y) \leq 0.5 \quad (17)$$

After imposing the above constraint, the optimum is found to be near the edge of a feasible band, which makes it a challenging problem as it is no longer smooth near the optimum. In this case, as an optimizer has little knowledge about the feasible band, it is inclined to consume execution budget on probing the feasible boundary whilst searching for the optimum.

In this simulation, we first investigate the behavior of DCBO without the additional constraint Eq. (17). In this setting, an algorithm is facing a squared feasible region, and it needs to make a recommendation within fifty trials, which is normally tight for an optimization problem. An execution trace is depicted in Fig. 5. It is interesting to note two properties on its behavior: (1) The algorithm began with a random search for the global optimum by aimless probing

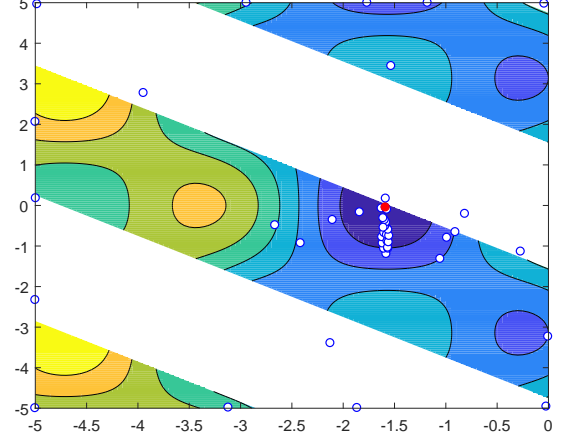


Fig. 6. The DCBO traces under a constraint. The blank areas indicate the infeasible regions. As before, fifty evaluations in total were allowed. We can observe that the directional constraint has a benefit to make new samples be prone to stay in the feasible region without asking for an explicit condition of feasibility.

on a 2D response surface. This is common in all Bayesian optimizations due to current lack of knowledge. (2) However, as the algorithm run, it learned about locations of probable optimum with a strong confidence. It fast concentrated its searching into the most possible areas. (3) In this example, besides the centric area it explored, it also searched the upper part since this also appears to be promising judged from history information. Its behavior exhibited jiggles since it had enough budget and directional constraint did not take great efforts in the beginning. DCBO erroneously converged to a local optimal point but managed to escape from it.

In Fig. 6, we elucidate an execution trace on the constrained problem. The effects of directional constraint on its behavioral aspects are more evident. The experimental setting keeps identical to the above example. From the figure, we can observe that: (1) This optimizer did not consider the upper part of figure as a promising area, so, in contrast to the above example, it did not take efforts to search for an optimum there. This phenomenon is not typical since each algorithm was initialized randomly. It devoted much of its model capacity to the centric region, which, as it appears, is the most promising area. The evaluation limit was relatively adequate when an optimizer happened to identify the best searching region. The redundant trials lead to more local searches. (2) A less noticeable phenomenon is that although it has an adequate budget, an optimizer has very few infeasible samples off the feasible boundaries. This is due to the correction on searching directions when an infeasible samples were made. This correction guarantees that the next sample is from a more judicious searching direction.

We will demonstrate in Fig. 7 that the above analyses are not special. As suggested in [8], median value would be a reasonable representative for the mass of the data. Since each algorithm was initialized independently and randomly, the execution traces exhibit disparities. Thus, the empirical distribution of the utility gap measurements is heavy-tailed. An appropriate representative in this case would be their median values. But for completeness, we also report the averaged values as in Fig. 7b.

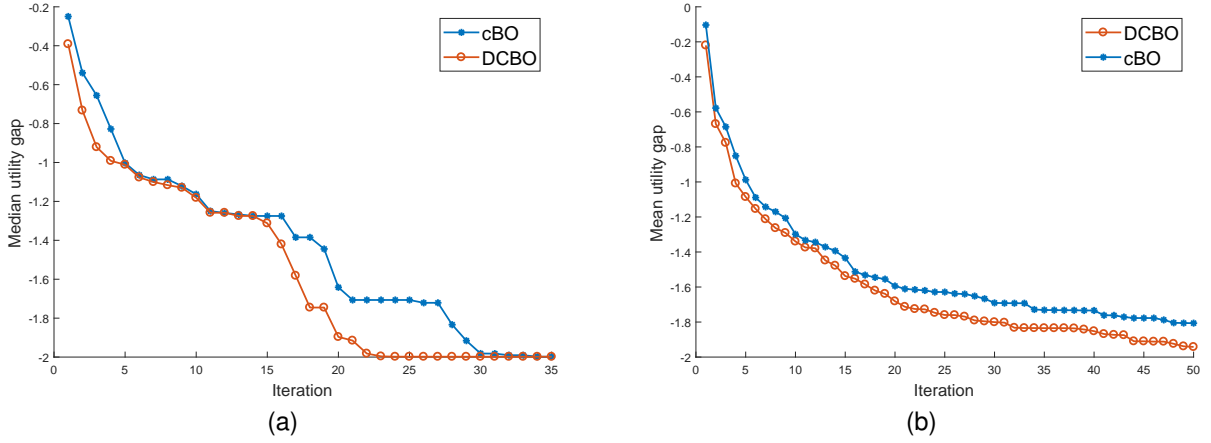


Fig. 7. (a): The comparison between cBO and DCBO in terms of median utility gap metric over 50 runs. For clarity, we only display the results up to 35 iterations. The curves indicate that both optimization policies behave similarly from the beginning. However, as the DCBO integrates additional directional knowledge inferred from its past samples, it gains a relative advantage, thus leading to a better overall performance. (b): The comparison between cBO and DCBO in terms of mean utility gap metric. The result shows that the directional constraint tends to increase the probability for an algorithm to return a better recommendation under a given evaluation budget.

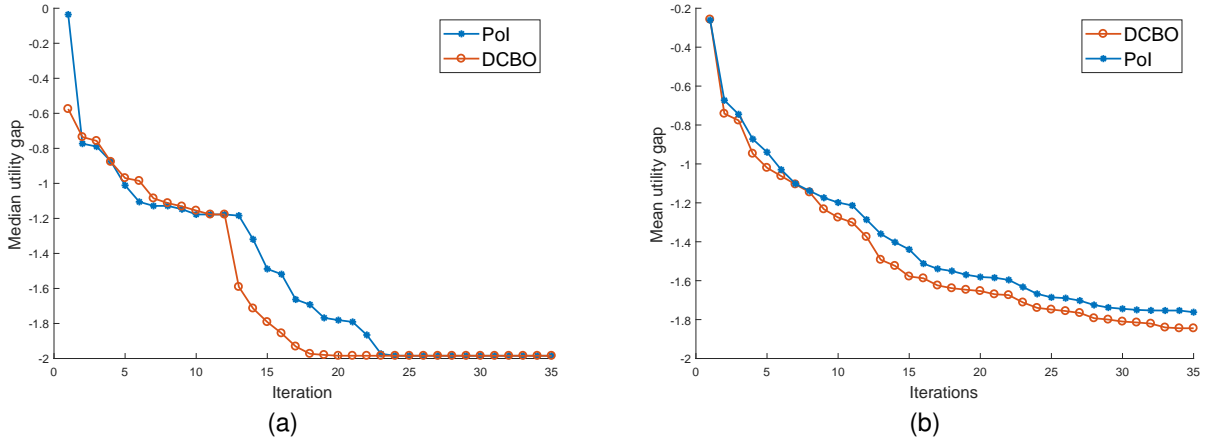


Fig. 8. (a): The comparison between Pol and DCBO in terms of median utility gap measures over 50 runs. The curves demonstrate that, after an initial search, DCBO can arrive at the global optimal point more quickly than Pol. (b): The comparison between Pol and DCBO in terms of mean utility gap measures.

In this simulation, we first compare the performances between constrained Bayesian optimization (cBO) [14] and DCBO proposed in our study. The former approach, cBO, is specially proposed for such an optimization problem under inequality constraints and has been served as a benchmark.

By looking into Fig. 7a, the curve exhibits a typical behavior of DCBO. As expected, the first half part (before iteration 15), both two curves have a highly similar behavior. In this stage, both are concentrating on exploring the unknown regions. After uncertainty over the response surface has been reduced significantly, DCBO decreases more quickly than its counterpart, achieving an overall advantage within the evaluation budget. Its counterpart, cBO, experiences two more plateaus before it reaches at optimal point. The plateaus, if shown in a figure, represents the inefficient jiggles on the response surface. A similar result in Fig. 7b demonstrates that DCBO achieves a consistent advantage over cBO as the two algorithms run.

In addition to the comparison with cBO, we also conduct the experiment between Probability of Improvement (Pol)

and DCBO on the unconstrained problem. Pol is a sampling policy that selects the next sample according to the probability of possible improvement brought by a candidate point. We evaluated Pol and DCBO on the problem as described by Eq. (16) but without constraint as Eq. (17). The total evaluation budget is still fifty times.

The experimental results are shown in Fig. 8. In Fig. 8a, a considerable speed-up is achieved as compared with the Pol. The behavioral aspects are analogous to that in Fig. 7a. The mean curves in Fig. 8b report a similar result. In current experimental settings with a limited evaluated budget, DCBO is superior to Pol.

Simulation 3

In this simulation, we examine the approximated solution provided as in Eq. (14) and the one estimated from sampled data. We check whether the technique of approximation may result in a performance degradation and thus slow down the optimization progress. Rather than assuming the form of probability distribution of directional data and making an approximation such that the posterior probabil-

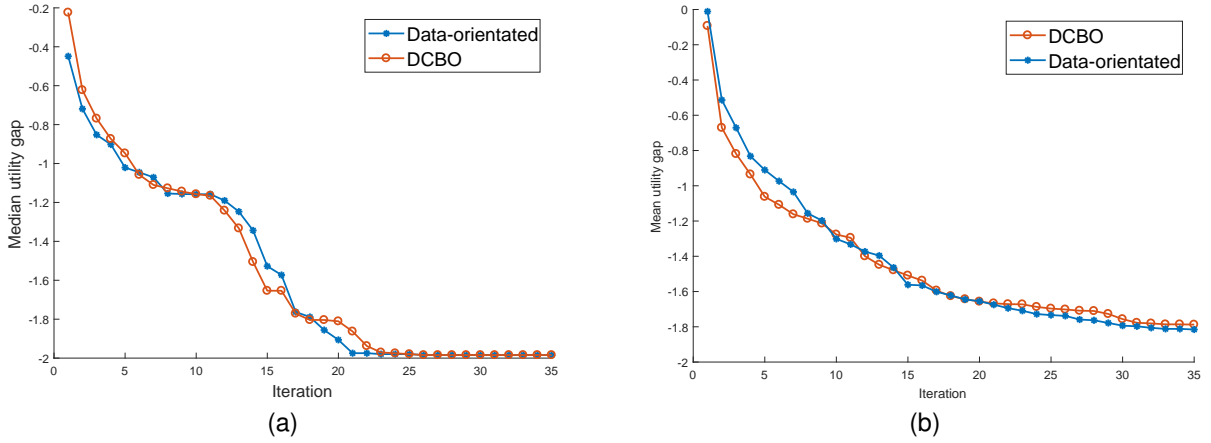


Fig. 9. (a): The comparison between the data-orientated approach and the DCBO in terms of median values of utility gaps. (b): The comparison between the data-orientated approach and the DCBO in terms of mean values of utility gaps. From this comparison, we know that two approaches have quite a close behavior in most cases. More details on set-up can be found in the text.

ity still keeps tractability, we drop these assumptions and directly estimate the necessary quantities from observations.

In this simulation, at time t , we sample a “best” point x^* according to its posterior distribution inferred from GP. Every x^* will result in a possible direction starting from current point x_t . If it spans a acute angle with the previous searching direction, this one is accepted, otherwise dropped. This procedure is repeated for 1000 times. The directional estimations are numerical normalized and interpolated over all directions. As indicated above, this method is numerical expensive and has a low efficiency.

The approaches to be compared are: (1) the approximation approach that is developed based on Bayesian formalism, that is, the DCBO; (2) the approach that have its posterior distribution numerically estimated via the sampling, which we call data-oriented approach. The experimental results of two approaches are displayed in Fig. 9. Their performances are measured through the median and the mean values of utility gaps. By checking the two figures, we can see that, although data-orientated approach does not have hypotheses on the form of posterior probability and interpolates probabilistic quantities using expensive numerical samplings, there is no significant advantage over DCBO, which is developed based on the approximation. Moreover, as shown in Fig. 9a, two curves exhibit a nearly identical tendency and are quite close to each other, representing that, in most cases, DCBO behaves almost the same as the data-orientated approach. A same analysis is also applicable to Fig. 9b.

4.3 Benchmark task

We assess DCBO by learning latent (hidden) parameters for linear dynamical system (LDS). Because of its mathematical analyzable structure, and predicative behavior, a time-invariant discrete LDS is arguably the most commonly used model for real-world engineering applications. Many physical systems could be accurately described by this model. The exact inference within the LDS can be done via Expectation Maximum based (EM-based) approaches. EM is an iterative optimization algorithm which requires many iterations to

converge. During each iteration, an algorithm needs to pass over the entire dataset. Hence, EM-based algorithms do not scale well to very long observations. Moreover, the parameter optimization in EM use either gradient descent or its variants and also needs many iterations to converge. These two factors together make EM-based approaches impractical for large dataset.

In this real-world application, we adopt an EM-based approximation method called Approximate Second-Order Statistics (ASOS) for learning the parameters of an LDS. This method was designed to trade-off a high-quantified solution against a speed-up on execution, which is controlled by a meta-parameter *klim*. This parameter has a broad feasible region. We restrict our attention to *klim* and the latent space dimension, as both are critical in determining its model capability. Carefully tuning these parameters can be prohibitively expensive. In contrast to the previous simulations, this problem is a discrete optimization problem.

In this experiment, EM-based approach was tested on a parametric combination and returns its negative log likelihood. This quantity measures the utility of this combination. As EM-based algorithm is low efficient, in our experimental setting, the maximum permitted number of executions is 50 times. An optimizer that quickly converged to a low negative log likelihood was valued high. All runs were initialized with different initial parameters, which were generated randomly and projected into their feasible regions. The optimization were repeated for fifty times. The mean values of utility gaps, as well as standard deviations, were collected and reported. As described in [22], every 10 iterations, an exact log likelihood was computed to revise the approximated ones.

We compared DCBO against several searching policies: PoI, EI, UCB with various κ . Some of them are among widely-used policies in real-world applications, due to their simplicity on conception and predictive behaviors. In particular, UCB leaves this task of trade-off to practitioners. Its parameter κ changes the proportion of exploration in one search. We vary this parameter in a representative set $\{0.5, 1, 6, 9\}$. Larger value means more exploration for UCB.

We adopt two real-world datasets. The first we used

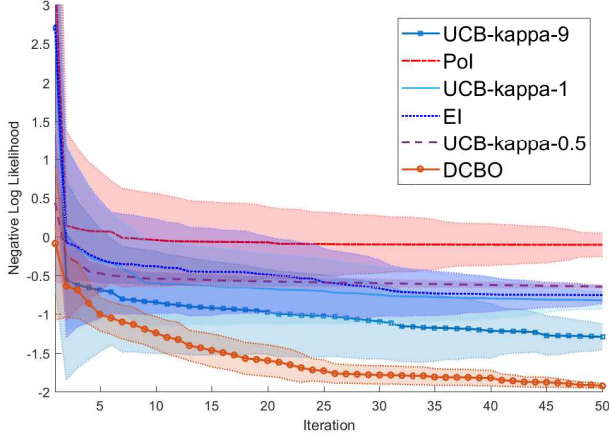


Fig. 10. The negative log likelihood returned by Bayesian searching policies. They are executed on the task of inferring the parameters for an LDS on the first dataset, *milk*. The mean and standard deviation are reported for each searching policy. On this challenging discrete optimization problem, DCBO reports a superior performance in recommending better parametric combinations for the LDS. From the figure, many searching policies are hindered by flat optimization plateaus and slow down. DCBO, however, keeps a steady decreasing tendency even in comparison with UCB-kappa-9 which spends more on exploration.

in our experiment was a 3-dimensional sequential data of length 6305. This dataset¹ was collected by sensors from an industrial milk evaporator. The second dataset is transformed sensor readings of length 15300 on motion capture. We used the first ten dimensions of this 49-dimensional dataset². Two datasets are referred to as *milk* and *motion*, respectively.

The experimental results are shown in Fig. 10 and Fig. 11. The lines summarize the statistics of utility gap metrics. Both the mean and standard variance are presented in the figures. For the clarity of presentation, we only draw the most three typical lines of UCB. From the two figures, we can conclude that, within all the comparison algorithms, DCBO can return the best parametric combination within a prescribed evaluation budget. Moreover, its negative log likelihood decreases more rapidly than its comparison algorithms. This means that its advantage appears not only in the end of execution, but also arises over most iterations. The comparison on standard deviations shows that in a majority of cases, DCBO performs well and can lead to a consistent decrease. This observation agrees with our primal goal in setting up the directional constraints.

5 CONCLUSION

In conclusion, there are many practical scenarios that standard Bayesian algorithm is ill-suited for. This is because it does not find a way to cast the realistic constraints like evaluation budget into the acquisition function in order to deal with the trade-off between speedup and the gradually tighten ambient budget.

1. This dataset is a standardly used for identifying a system and can be accessed via <http://homes.esat.kuleuven.be/~smc/daisy/daisydata.html>.

2. This dataset is available on-line from <http://mocap.cs.cmu.edu/>. The preprocessing step was described as in [23]

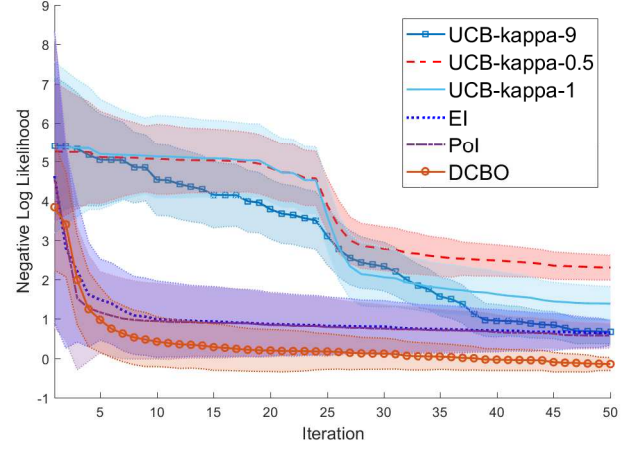


Fig. 11. The negative log likelihood returned by Bayesian searching policies. They are executed on the task of inferring the parameters for an LDS on the second dataset, *motion*. On this dataset, DCBO is the most effective one. Although UCB-kappa-9 finally achieves a comparable result, it has a large deviation and experiences a long stagnation where no significant progress is made. EI and Pol have analogous traces and nearly overlap each other. Not surprisingly, DCBO preserves their major features on shapes but accelerates the decreasing pace.

An optimizer needs to be aware of the remaining evaluation budget. To do so, we generalize the standard Bayesian optimization and propose a multiplicatively reweighed searching policies, combining both global and local strategies. On the local scale, we use a directional constraint to assist the optimizer, which can be easily adapted into other probabilistic Bayesian optimization frameworks as a plug-in module. This strategy performs well in reducing the jiggles exhibited in standard expected improvement. The studies in real-world applications demonstrate that this method could have substantial speedup without violating the prescribed evaluation limitation.

Hitherto, we discuss the possibility of conducting Bayesian optimization in a scenario with limited evaluation budget. However, there are prior knowledges that are hard to be described in terms of probabilities. For instance, the partial order existing among parameters and constraints on the parametric magnitude. In addition, there exist a power in our formulation of the new acquisition function, which controls the relative importance between two factors. This power is considered to be a nuisance parameter. It is desirable for an adaptive function that can automatically tune the balance between two factors. Both problems need more complicated techniques, which constitute our future work.

APPENDIX

The directional constraint for any given x takes a probabilistic form, with the direction ending at x as its argument. From the Bayesian formalism, we need to infer its posterior probability under an acute angle restriction. The update rule for the posterior probability takes the following form:

$$\begin{aligned} H_{t+1}(x) &= p(g_{t+1}) \\ &= \int dg_t^* dg_t \mathbb{I}(\langle g_{t+1}, g_t \rangle \geq 0) p(g_t) p(g_{t+1} | g_t^*) p(g_t^*) \end{aligned} \quad (18)$$

where $g_{t+1} = \frac{x - x_t}{\|x - x_t\|}$.

To solve Eq. (18), we need to infer $p(g^*)$ from the GP which takes the form of a Gaussian distribution. This transformation extracts directional uncertainties from the statistics of x^* . Suppose we have the posterior estimation at the position x^* :

$$p(x^*) = \mathcal{N}(\mu_{x^*}, \Sigma_{x^*}) \quad (19)$$

Define a series of N samples \mathbf{x}_i draw from Gaussian distribution $\mathbf{x}_i, i = 1, \dots, N$. Following [20], [21], we know immediately that the maximum likelihood estimation of θ and κ are give by

$$\begin{cases} \theta = \frac{\sum_{i=1}^N \mathbf{x}_i}{\|\sum_{i=1}^N \mathbf{x}_i\|} \\ \kappa = A_d^{-1}(\frac{1}{N} \|\sum_{i=1}^N \mathbf{x}_i\|) \end{cases} \quad (20)$$

where $A_d = \frac{B_{d/2}(\kappa)}{B_{d/2-1}(\kappa)}$.

Introducing an intermediate variable $R = \frac{1}{N} \|\sum_{i=1}^N \mathbf{x}_i\|$, [21] points out a simple approximation to κ by

$$\kappa = \frac{R(d - R^2)}{1 - R^2} \quad (21)$$

Suppose we adopt an Euclidean norm, the estimation of R could be easily obtained through samples from the Gaussian distribution $p(x^*)$.

$$\hat{R} = \frac{1}{N} \mathbb{E} \sqrt{\left(\sum_{i=1}^N \frac{\mathbf{x}_i}{\|\mathbf{x}_i\|}\right)^T \left(\sum_{i=1}^N \frac{\mathbf{x}_j}{\|\mathbf{x}_j\|}\right)} \quad (22)$$

Notationally, a random variable with hat represents the one estimated through samples from a distribution. In summary, the key parameters in $p(g^*)$ are listed as follows:

$$\begin{cases} \hat{\theta} = \frac{\mu}{\hat{R}} \\ \hat{\kappa} = \frac{\hat{R}(d - \hat{R}^2)}{1 - \hat{R}^2} \end{cases} \quad (23)$$

Having obtained $p(g^*)$, the next step is to compute the integral. Since there is no closed-form solution, the posterior distribution needs to be carefully approximated. Provided that this posterior distribution is in the same family as the prior probability, such that the chain rule of Bayesian formalism could work.

The posterior probability of g_{t+1} is formulated as:

$$p(g_{t+1}|x_t, g^*) = Vmf(g_{t+1}|\theta_{t+1}, \kappa_{k+1})$$

where $\theta_{t+1} = g^* = \frac{\mu_{x^*} - x_t}{\|\mu_{x^*} - x_t\|}$.

From Eq. (18), we know that the posterior probability can be split into a product of two independent terms:

$$\begin{aligned} & p(g_{t+1}) \\ &= \int dg^* dg_t \mathbb{I}(\langle g_{t+1}, g_t \rangle \geq 0) p(g_{t+1}|g_t^*) p(g_t^*) \\ &= \int dg^* p(g_{t+1}|g_t^*) p(g_t^*) \int dg_t \mathbb{I}(\langle g_{t+1}, g_t \rangle \geq 0) p(g_t) \end{aligned}$$

Let us first concentrate on the first term in the above product.

$$\begin{aligned} & \int dg^* p(g_{t+1}|g_t^*) p(g_t^*) \\ &= \int_{\|g^*\|=1} dg^* p(g_t|g^*, x_t) p(g^*|x_t) \\ &= \int_{\|g^*\|=1} dg^* Vmf(g_{t+1}|g^*, \kappa_t) Vmf(g^*|\hat{\theta}^*, \hat{\kappa}^*) \\ &= C_d(\kappa_t) C_d(\hat{\kappa}^*) \int_{\|g^*\|=1} \exp(\kappa_t g^{*T} g_{t+1} + \hat{\kappa}^* g^{*T} \hat{\theta}^*) \\ &= C_d(\kappa_t) C_d(\hat{\kappa}^*) \int_{\|g^*\|=1} \exp((\kappa_t g_{t+1} + \hat{\kappa}^* \hat{\theta}^*)^T g^*) \end{aligned}$$

where we include stationary points for ease of understanding.

We use the fact that g_t is distributed according to Vmf of center θ_t and concentration parameter κ_t . The second term in the product can be computed as:

$$\begin{aligned} & \mathbb{E} \mathbb{I}(\langle g_{t+1}, g_t \rangle \geq 0) \\ &= \int_{g_{t+1} - \frac{\pi}{2}}^{g_{t+1} + \frac{\pi}{2}} Vmf(g_t|\theta_t, \kappa_t) dg_t \\ &= C \exp(\kappa_t \theta_t^T g_{t+1}) \end{aligned}$$

where the constant term C summarizes all irrelevant terms in terms of g_{t+1} . Here and subsequently, we write C to stand for the constant that are irrelevant to the variable of interest.

From the equality

$$\int_{\|\mathbf{x}\|=1} \exp(\kappa \theta^T \mathbf{x}) d\mathbf{x} = \frac{(2\pi)^{d/2-1} B_{d/2-1}(\kappa)}{\kappa^{d/2-1}} \equiv C_d(\kappa)$$

it may be concluded that

$$\begin{aligned} & p(g_{t+1}|x_t) \\ &= \mathbb{E} \mathbb{I}(\langle g_{t+1}, g_t \rangle \geq 0) C_d(\kappa_t) C_d(\hat{\kappa}^*) C_d(\|\kappa_t g_{t+1} + \hat{\kappa}^* \hat{\theta}^*\|) \\ &= C \exp(\kappa_t \theta_t^T g_{t+1}) C_d(\|\kappa_t g_{t+1} + \hat{\kappa}^* \hat{\theta}^*\|) \end{aligned}$$

As defined above, C is a generic constant term that varies in the context.

If we hope to build a hierarchy model as Bayesian optimization does, it is necessary to provide the posterior estimation for the κ . A well-known equality for distribution in exponential family states that:

$$\frac{\partial \log p(x)}{\partial x} = \kappa \theta \quad (24)$$

Then, the parameter κ_{t+1} are approximated with the following equations.

$$\begin{aligned} & \frac{\partial}{\partial g_{t+1}} \log p(g_{t+1}) \\ &= \frac{\partial}{\partial g_{t+1}} \log (C \exp(\kappa_t \theta_t^T g_{t+1}) C_d(\|\kappa_t g_{t+1} + \hat{\kappa}^* \hat{\theta}^*\|)) \\ &= \frac{\partial}{\partial g_{t+1}} \log C_d(\|\kappa_t g_{t+1} + \hat{\kappa}^* \hat{\theta}^*\|) + \kappa_t \theta_t \end{aligned}$$

This is not a properly defined statistical quantity, but we approximate this quantity with probability in the same family. After defining an intermediate variable $y = \|\kappa_t g_{t+1} +$

$\hat{\kappa}^* \hat{\theta}^*$, we approximate it with the Taylor series in terms of g_{t+1} , which can be obtained as:

$$y = \sqrt{\hat{\kappa}^{*2} + \kappa_t^2} + \frac{\hat{\kappa}^* \kappa_t \hat{\theta}^* g_{t+1}}{\sqrt{\hat{\kappa}^{*2} + \kappa_t^2}} + \frac{(\hat{\kappa}^* \kappa_t \hat{\theta}^*)^2 g_{t+1}^2}{2(\hat{\kappa}^{*2} + \kappa_t^2)^{3/2}} + O(g_{t+1}^3) \quad (25)$$

Taking derivative on both sides of Eq. (25) with respect to g_{t+1} , we get

$$\frac{dy}{dg_{t+1}} = \frac{\hat{\kappa}^* \kappa_t \hat{\theta}^*}{\sqrt{\hat{\kappa}^{*2} + \kappa_t^2}} + \frac{(\hat{\kappa}^* \kappa_t \hat{\theta}^*)^2 g_{t+1}}{(\hat{\kappa}^{*2} + \kappa_t^2)^{3/2}} + O(g_{t+1}^2) \quad (26)$$

We notice that the function $\log C_d(y)$ could be decomposed as follows:

$$\begin{aligned} \log C_d(y) &= \log \frac{(2\pi)^{d/2-1} B_{d/2-1}(y)}{y^{d/2-1}} \\ &= \left(\frac{d}{2} - 1\right) \log 2\pi + \log B_{\frac{d}{2}-1}(y) - \left(\frac{d}{2} - 1\right) \log y \end{aligned} \quad (27)$$

Again, taking derivative on both sides of Eq. (27), we get

$$\begin{aligned} \frac{d}{dy} \log C_d(y) &= -\left(\frac{d}{2} - 1\right) \frac{1}{y} + \frac{d}{dy} \log B_{\frac{d}{2}-1}(y) \\ &\approx \frac{y}{d} - \frac{y^3}{d^2(d+2)} + O(y^4) \end{aligned} \quad (28)$$

during which, we make use of an equality

$$\frac{d}{dy} \log B_{\frac{d}{2}-1}(y) = \frac{B_{\frac{d}{2}}(y) + B_{\frac{d}{2}-2}(y)}{2B_{\frac{d}{2}-1}(y)}$$

and expand the results in a Taylor series.

Put Eq. (26) and Eq. (28) together, we get

$$\begin{aligned} \frac{d}{dy} C_d(y) \frac{dy}{dg_{t+1}} &= -\frac{\hat{\kappa}^* \kappa_t \hat{\theta}^* (-d(d+2) + \hat{\kappa}^{*2} + \kappa_t^2)}{d^2(d+2)} + O(g_{t+1}) \\ &\approx -\frac{\hat{\kappa}^* \kappa_t \hat{\theta}^* (-d(d+2) + \hat{\kappa}^{*2} + \kappa_t^2)}{d^2(d+2)} \\ &\triangleq k_1 \hat{\theta}^* \end{aligned}$$

where the third equality uses the fact that $\|\hat{\theta}^*\| = 1$. In the fourth equation, we introduce two intermediate variables:

$$k_1 = -\frac{\hat{\kappa}^* \kappa_t (-d(d+2) + \hat{\kappa}^{*2} + \kappa_t^2)}{d^2(d+2)}$$

By the fact that $\|\theta_{t+1}\| = 1$, we reach the final update rules:

$$\begin{cases} \kappa_{t+1} = \sqrt{k_1^2 + \kappa_t^2} \\ \theta_{t+1} = \frac{1}{\kappa_{t+1}} k_1 \hat{\theta}^* + \frac{1}{\kappa_{t+1}} \kappa_t \theta_t \end{cases} \quad (29)$$

REFERENCES

- [1] J. Moćkus, "On bayesian methods for seeking the extremum," in *Optimization Techniques IFIP Technical Conference*. Springer, 1975, pp. 400–404.
- [2] D. R. Jones, "A taxonomy of global optimization methods based on response surfaces," *Journal of global optimization*, vol. 21, no. 4, pp. 345–383, 2001.
- [3] N. Srinivas, A. Krause, S. Kakade, and M. Seeger, "Gaussian process optimization in the bandit setting: No regret and experimental design," in *International Conference on International Conference on Machine Learning*, 2010, pp. 1015–1022.
- [4] H. J. Kushner, "A new method of locating the maximum point of an arbitrary multipeak curve in the presence of noise," *Journal of Basic Engineering*, vol. 86, no. 1, pp. 97–106, 1964.
- [5] N. Srinivas, A. Krause, S. M. Kakade, and M. W. Seeger, "Information-Theoretic Regret Bounds for Gaussian Process Optimization in the Bandit Setting," *IEEE Transactions on Information Theory*, vol. 58, no. 5, pp. 3250–3265, May 2012.
- [6] A. D. Bull, "Convergence rates of efficient global optimization algorithms," *Journal of Machine Learning Research*, vol. 12, no. Oct, pp. 2879–2904, 2011.
- [7] P. Hennig and C. J. Schuler, "Entropy search for information-efficient global optimization," *Journal of Machine Learning Research*, vol. 13, no. Jun, pp. 1809–1837, 2012.
- [8] J. M. Hernández-Lobato, M. A. Gelbart, M. W. Hoffman, R. P. Adams, and Z. Ghahramani, "Predictive Entropy Search for Bayesian Optimization with Unknown Constraints," in *International Conference on Machine Learning*, vol. 37, 2015, pp. 1699–1707.
- [9] D. Hernández-Lobato, J. M. Hernández-Lobato, A. Shah, and R. P. Adams, "Predictive Entropy Search for Multi-objective Bayesian Optimization," in *International Conference on Machine Learning*, vol. 48, 2016, pp. 1492–1501.
- [10] C. M. Bishop, *Pattern Recognition and Machine Learning*. Springer, 2006, vol. 4, no. 4.
- [11] C. E. Rasmussen and C. K. I. Williams, *Gaussian processes for machine learning*, ser. Adaptive computation and machine learning. Cambridge, Mass: MIT Press, 2006.
- [12] E. Brochu, V. M. Cora, and N. de Freitas, "A Tutorial on Bayesian Optimization of Expensive Cost Functions, with Application to Active User Modeling and Hierarchical Reinforcement Learning," *arXiv:1012.2599 [cs]*, Dec. 2010.
- [13] D. R. Jones, M. Schonlau, and W. J. Welch, "Efficient Global Optimization of Expensive Black-Box Functions," *Journal of Global Optimization*, vol. 13, no. 4, pp. 455–492, Dec. 1998.
- [14] J. R. Gardner, M. J. Kusner, Z. E. Xu, K. Q. Weinberger, and J. P. Cunningham, "Bayesian Optimization with Inequality Constraints," in *International Conference on Machine Learning*, 2014, pp. 937–945.
- [15] V. Picheny, R. B. Gramacy, S. M. Wild, and S. L. Digabel, "Bayesian optimization under mixed constraints with a slack-variable augmented Lagrangian," in *Advances in Neural Information Processing Systems*, 2016, pp. 1435–1443.
- [16] J. Bernardo, M. J. Bayarri, J. O. Berger, A. P. Dawid, D. Heckerman, A. F. M. Smith, and M. West, "Optimization under unknown constraints," *Bayesian Statistics*, vol. 9, no. 9, p. 229, 2011.
- [17] V. Picheny, "A Stepwise uncertainty reduction approach to constrained global optimization," in *Artificial Intelligence and Statistics*, Apr. 2014, pp. 787–795.
- [18] R. Lam and K. Willcox, "Lookahead Bayesian Optimization with Inequality Constraints," in *Advances in Neural Information Processing Systems*, I. Guyon, U. v. Luxburg, S. Bengio, H. M. Wallach, R. Fergus, S. V. N. Vishwanathan, and R. Garnett, Eds., 2017, pp. 1888–1898.
- [19] R. Lam, K. Willcox, and D. H. Wolpert, "Bayesian optimization with a finite budget: An approximate dynamic programming approach," in *Advances in Neural Information Processing Systems*, 2016, pp. 883–891.
- [20] S. R. Jammalamadaka and A. Sengupta, *Topics in circular statistics*, ser. Series on multivariate analysis. River Edge, N.J.: World Scientific, 2001, no. v. 5.
- [21] A. Banerjee, I. S. Dhillon, J. Ghosh, and S. Sra, "Clustering on the Unit Hypersphere Using Von Mises-Fisher Distributions," *J. Mach. Learn. Res.*, vol. 6, pp. 1345–1382, Dec. 2005.
- [22] J. Martens, "Learning the linear dynamical system with ASOS," in *International Conference on Machine Learning*, 2010, pp. 743–750.

- [23] G. W. Taylor, G. E. Hinton, and S. T. Roweis, "Modeling human motion using binary latent variables," in *Advances in neural information processing systems*, 2007, pp. 1345–1352.